

SPECTRAL AND LUMINESCENT PROPERTIES OF DOPED FLUROALUMINATE GLASSES PROMISING FOR OPTICAL TEMPERATURE SENSORS

V.A. Klinkov

Peter the Great St. Petersburg Polytechnic University, St. Petersburg, Russian Federation

Spectral and luminescent properties of Er^{3+} -doped fluoroaluminate glasses have been studied and presented in the paper. The subject of inquiry was $98\text{MgCaSrBaYAl}_2\text{F}_{14}-2\text{Ba}(\text{PO}_3)_2$ glass, the ErF_3 concentrations were of 0.1 – 1.0 mol. %. The optical absorption spectra were analyzed in the range from 190 to 1700 nm, and the nature of absorption bands was explained on a basis of the Er^{3+} ion energy diagram. The up-conversion spectra were measured at 77 and 300 K in the 500 – 700 nm range upon 975 nm laser excitation. The temperature dependences of FIR were calculated using the experimental data in a range of (77 – 300) K. Among the samples under investigation the 0.1% ErF_3 one possessed the greatest response to temperature changes in the range of (77 – 300) K. The studied material was proved to be a candidate for realizing the optical temperature sensors.

Key words: optical temperature sensor; rare-earth ion; absorption spectrum; luminescence; fluoroaluminate glass

Citation: V.A. Klinkov, Spectral and luminescent properties of doped fluoroaluminate glasses promising for optical temperature sensors, St. Petersburg State Polytechnical University Journal. Physics and Mathematics. 11 (1) (2018) 33 – 40. DOI: 10.18721/JPM.11105

Introduction

To date, numerous applied and fundamental have been aimed at synthesizing new glassy materials for the near and mid infrared (IR) ranges, since the currently available materials are limited. Vibrational-rotational absorption bands of most molecules and chemical compounds are located within these spectral ranges, making them detectable by IR spectroscopy [1].

The materials of the mid IR range include non-oxide glasses, in particular, fluoride and chalcogenide. The latter are characterized not only by a wider bandwidth of electromagnetic radiation in the IR region than quartz glasses, but also by lower optical losses (this was proved by theoretical studies) [2]. Optical fiber amplifiers and fiber lasers based on non-oxide glass doped with rare earth elements have a significant practical significance for telecommunication lines [3]. It is non-oxide glasses that have an important distinctive characteristic: their high-frequency boundary of the vibrational spectrum is substantially lower than that of oxide glasses; as a consequence, the probability of intracenter nonradiative processes decreases [4] and the quantum yield of the luminescence of

the dopants introduced into the glass matrix increases. In addition, laser electron transitions, which are quenched by thermal lattice vibrations of the glassy matrix in oxide glasses, can be achieved in non-oxide fluoride and chalcogenide glasses.

Non-oxide glasses doped with trivalent ions of rare earth elements are studied for potential applications in near and mid-IR lasers [4], fiber lasers [5], fiber amplifiers [6] and optical sensors [7, 8]. In particular, glasses doped with erbium ions (Er^{3+}) were used to create optical fiber amplifiers for fiber optic communication lines and optical temperature sensors [9], operating on the principle of upconversion luminescence using the FIR (Fluorescence Intensity Ratio) technique; these devices are an alternative to quartz-based ones.

The main advantages of optical temperature detectors over classical contact methods of measurement is that they have a high temperature sensitivity and low inertia, small sizes, electromagnetic passivity and high noise immunity, and they can be used in extreme environmental conditions [10]. To date, the choice of a glassy matrix for optical temperature sensors remains an open problem, but it was established in [11] that the glassy matrix plays a key role in the

sensitivity of optical temperature sensors: the best results have been obtained for glassy systems with lower values of the high-frequency boundary of the vibrational spectrum.

Thus, from the standpoint of their luminescent properties (in particular, taking into account the phenomenon of upconversion luminescence), chalcogenide and fluoride glasses can be considered to be the most promising for creating optical temperature sensors.

The disadvantages of chalcogenide glasses include low chemical and thermal stability, toxicity, incompatibility with quartz glasses in terms of the refractive index ($n > 2.2$) and the thermal parameters, complicated synthesis and low solubility of active impurities such as transition and rare earth elements.

Fluoride glasses allow introducing high concentrations of rare-earth dopants, have a refractive index close to quartz fiber ($n \approx 1.5$), high thermal stability and a wide transparency range (from 0.25 to 8.00 μm), which makes them the best glassy materials for applications in active optical media for the mid-IR range.

The spectral and luminescent properties of fluoroaluminate $98\text{MgCaSrBaYAl}_2\text{F}_{14}-2\text{Ba}(\text{PO}_3)_2$ glasses doped with erbium ions (Er^{3+}) have been investigated in this study; the upconversion luminescence spectra obtained at temperatures of 77 and 300 K have been recorded and interpreted.

The intensity ratios of the fluorescence bands generated by energy transitions from the thermally coupled levels to the ground state were calculated on the basis of the experimental data for the temperature range of 77 – 300 K. According to the data available in the literature, the glasses of this composition with this dopant were not previously studied as sensitive elements for upconversion temperature sensors.

The composition of the glass was chosen taking into account the results obtained earlier in [12, 13]. In particular, glasses with the selected composition exhibit reduced crystallization ability, high homogeneity and minimum content of OH groups, as well as a wide pass-band up to 6.4 μm .

Experimental procedure

The glasses were synthesized in an SU-2000 crucible of for 1 h at temperatures of

Table

Dopant contents in fluoride $98\text{MgCaSrBaYAl}_2\text{F}_{14}-2\text{Ba}(\text{PO}_3)_2$ glasses and sample notations

Er^{3+} content, mol %	Sample notation
0.1	0.1 % ErF_3
0.5	0.5 % ErF_3
1.0	1.0 % ErF_3

Note. The dopant was introduced into the glassy matrix through erbium fluoride ErF_3 in excess of 100 mol%.

850 – 950 ° C, without stirring the glass melt, in an argon atmosphere. The glass was melted in an inert argon atmosphere to prevent impurities, particularly, water, iron and hydroxyl groups, from entering the melt from the surrounding air. Erbium fluoride was introduced in excess of 100 mol%. The glass samples obtained this way were cut into 1-mm-thick plane-parallel plates, ground and polished. Compositions and names of the glass samples are given in the Table.

The optical absorption spectra were recorded with a Lambda 900 spectrophotometer (Perkin-Elmer LLC, USA) at room temperature (300 K).

The pumping radiation source was a Ti:sapphire laser with a working wavelength $\lambda = 975$ nm (the Spectra Physics Model 3900) operating in continuous mode. Luminescence spectra in the 450 – 900 nm range were recorded with a highly sensitive AvaSpec-2048 USB2 fiber-optic spectrometer, an Acton-300 monochromator and an ID-441 receiver (Acton Research Corporation). A GS21525 variable temperature cell holder with optical windows (Specac), paired with a diffusion pump, was used for low-temperature measurements.

Results and discussion

Fig. 1 shows the optical absorption spectra of fluoroaluminate glass samples in the 190 – 1700 nm range. The bands observed in this range correspond to the $4f^{11} \rightarrow 4f^{11}$ intraconfiguration transitions from the $^4I_{15/2}$ ground state to the excited states of Er^{3+} , with the position of the maxima of these bands corresponding to the well-known Dicke diagram [14].

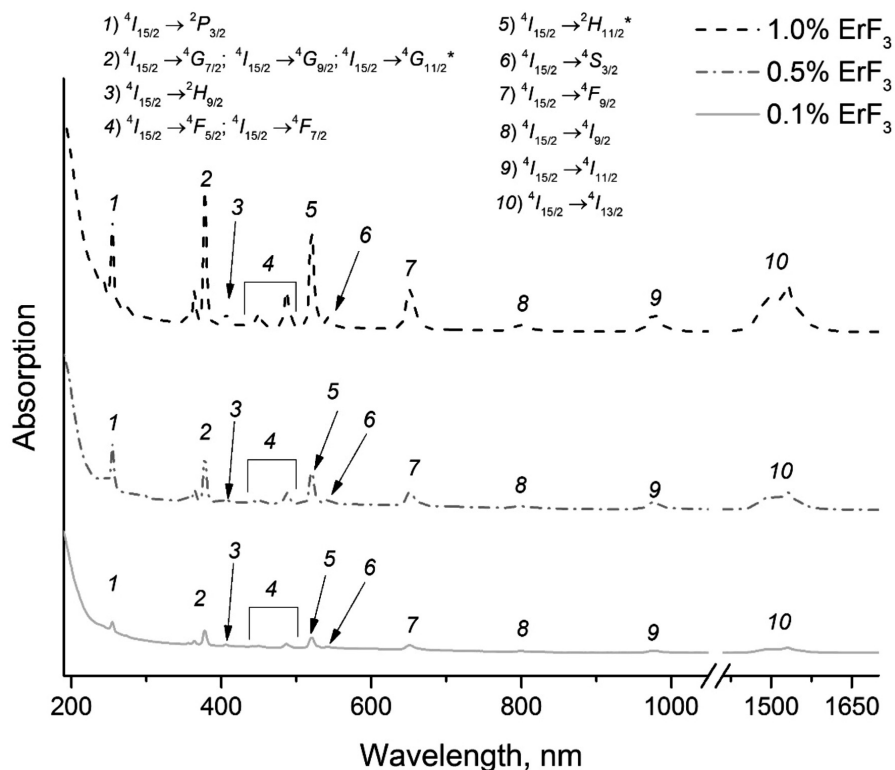


Fig. 1. Optical absorption spectra of fluoroaluminate glass samples of (0.1 – 1.0) % ErF_3 in the 190 – 1700 nm range.

The asterisks mark the hypersensitive transitions ${}^4I_{15/2} \rightarrow {}^2H_{11/2}$ and ${}^4I_{15/2} \rightarrow {}^4G_{11/2}$

The most intense and wide absorption bands have maxima at about 378, 487, 521, 651, 976 and 1532 nm and correspond to transitions from the ${}^4I_{15/2}$ ground state to the ${}^4G_{11/2}$, ${}^4F_{7/2}$, ${}^2H_{11/2}$, ${}^4F_{9/2}$, ${}^4I_{11/2}$ and ${}^4I_{13/2}$ levels, respectively. The positions of the absorption band maxima do not change with increasing dopant concentration and leads only to a relative increase in the absorption intensity, which may indirectly indicate a homogeneous distribution of the dopant.

To verify the agreement between the actual concentrations of the absorption centers (Er^{3+} ions) and the calculated values and to confirm the absence of dopant segregation in the glass [15], we have checked whether the Beer–Lambert–Bouguer law [16] was fulfilled for bands with the highest absorption coefficient values: 378, 521, 976 and 1532 nm (the positions of the maxima are indicated). The dependence of the absorption coefficients on the dopant concentration is shown in Fig. 2. The linear

dependence obtained confirms that this law is fulfilled and that the actual concentrations of

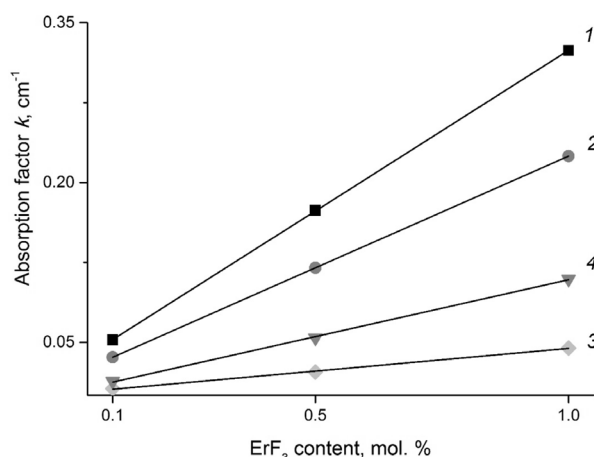


Fig. 2. Concentration dependences of the optical absorption coefficient for electron transitions at wavelengths of 378 nm (1), 521 nm (2), 976 nm (3) and 1532 nm (4) in fluoroaluminate glass samples activated by Er^{3+} ions

dopant ions agree with the calculated values.

The narrow and well-resolved absorption bands associated with the hypersensitive electron transitions $^4I_{15/2} \rightarrow ^2H_{11/2}$ and $^4I_{15/2} \rightarrow ^4G_{11/2}$ also indicate that the dopant distribution in the samples is homogeneous. Thus, analysis of the obtained optical absorption spectra showed that segregation effects are not observed

in the samples and there is no inhomogeneous broadening of the absorption bands. This indicates that an increase in the concentration of Er^{3+} ions does not lead to a disturbance of the glass structure and does not generate diverse local environments that Er^{3+} ions can occupy [17].

Fig. 3 shows the upconversion luminescence spectra

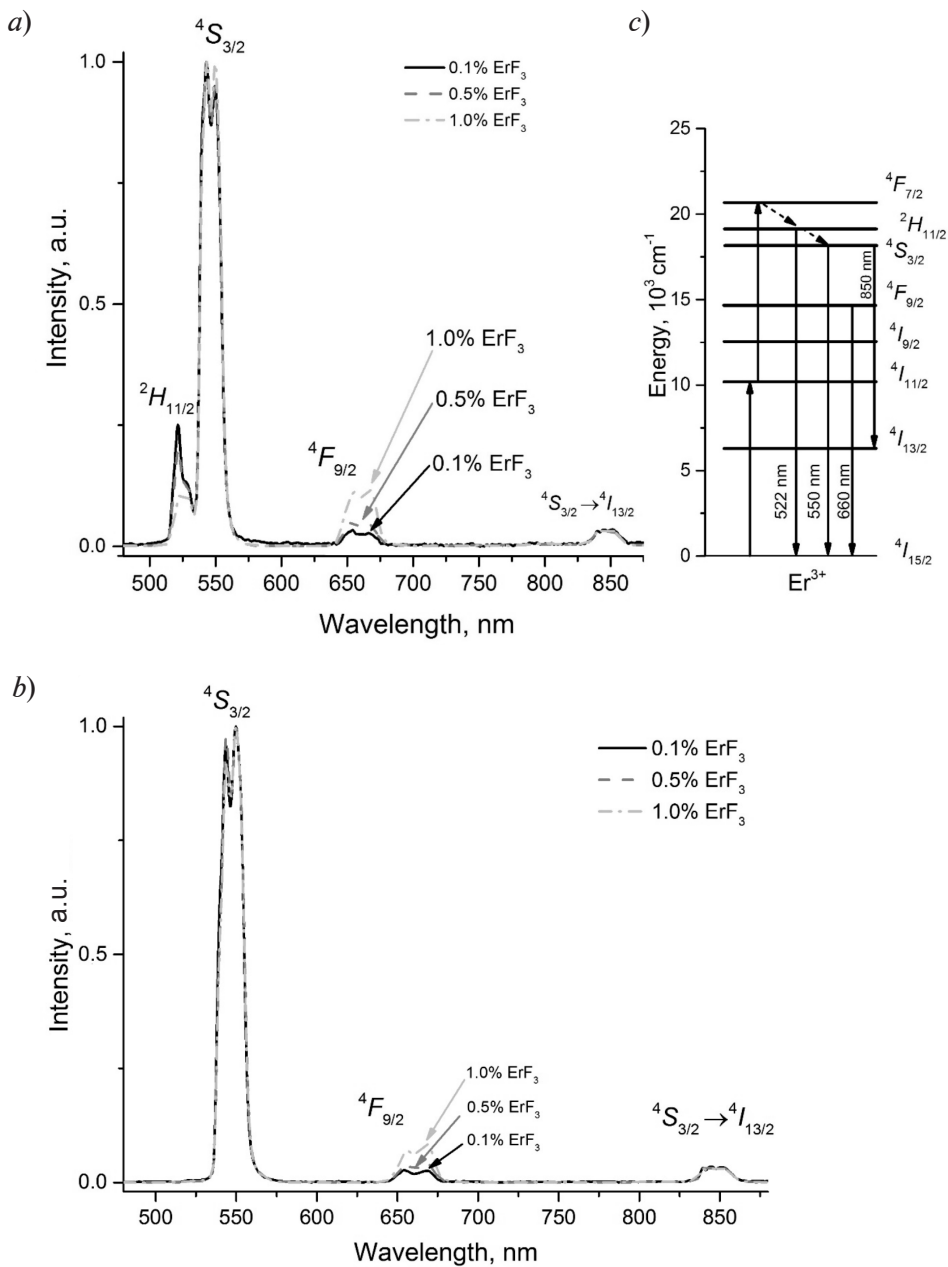


Fig. 3. Upconversion luminescence spectra of doped fluoroaluminate glass samples at 300 K (a) and 77 K (b); the luminescence intensities are normalized to the maximum intensity of each spectrum; the energy level diagram of the Er^{3+} ion and the excitation energy transfer mechanism (c) are given

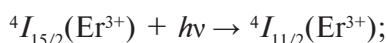
spectra of doped fluoroaluminate glass samples in the 450 – 900 nm range obtained by excitation with coherent radiation from a Ti:sapphire laser at a wavelength $\lambda = 975$ nm operating in continuous mode at temperatures of 300 and 77 K.

Let us consider the luminescence spectra obtained at 300 K (Fig. 3, *a*). The spectra include three groups of bands: with emission maxima around 522 and 550 nm in the green region, around 660 nm in the red region and around 850 nm in the near IR region.

The first group of bands is due to electron transitions from the ${}^2H_{11/2}$ (522 nm) and ${}^4S_{3/2}$ (550 nm) levels to the ${}^4I_{15/2}$ ground state. These levels are populated from the upper ${}^2F_{7/2}$ level by a mechanism of excitation energy transfer [13]. The energy level diagram of the Er^{3+} ion and the excitation energy transfer mechanism under pumping by laser radiation at a wavelength $\lambda = 975$ nm are shown in Fig. 3, *c*.

Let us consider the mechanism of excitation energy transfer in more detail. The mechanism includes ground state absorption (GSA), excited state absorption (ESA), and the exchange interaction. In view of these phenomena, the population of the ${}^4F_{7/2}$ level can occur by the following scheme:

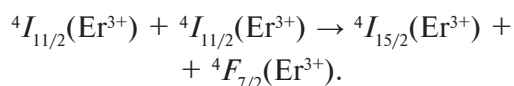
ground state absorption by the reaction



excited state absorption by the reaction



exchange interaction by reaction

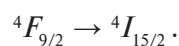


Next, non-radiative relaxation occurs from the ${}^4F_{7/2}$ level to the levels ${}^4H_{11/2}$ and ${}^4S_{3/2}$, and then a radiative transition to the ground state occurs by the scheme



while the luminescence peaks are positioned at wavelengths of about 522 and 550 nm, respectively.

The red luminescence band (660 nm) is associated with an electron transition



The population of the ${}^4F_{9/2}$ level occurs with the participation of the energy levels ${}^4F_{7/2}$, ${}^4H_{11/2}$ and ${}^4S_{3/2}$ above it through a non-radiative relaxation process. Due to the multistage nature of the population mechanism, the ${}^4F_{9/2}$ level is far less populated than the levels ${}^4H_{11/2}$ and ${}^4S_{3/2}$, which leads to a significantly lower relative intensity of the luminescence band with a maximum at about 660 nm.

The third luminescence band in the 850 nm region is due to the ${}^4S_{3/2} \rightarrow {}^4I_{13/2}$ electron transition. The presence of this band is important because in this case the transition is not from the excited state to the ground state but from the excited state to the non-ground state below it. The probability of this process is rather low, and the value of the high-frequency boundary of the vibrational spectrum of the glassy matrix is a factor considerably affecting the ${}^4S_{3/2} \rightarrow {}^4I_{13/2}$ transition. Notably, this band is found mainly in non-oxide glasses, in particular, in fluoride glasses [18].

Let us analyze the upconversion luminescence spectra obtained at a temperature of 77 K (Fig. 3, *b*). The same as at room temperature, three groups of bands can be observed on the spectra. The spectral positions of the luminescence band maxima are completely identical at 300 and 77 K. However, a significant decrease is observed in the intensity of the luminescence peak around 522 nm for all concentrations of the dopant. This phenomenon confirms the thermal nature of the population of the ${}^2H_{11/2}$ energy level. At room temperature, the ${}^2H_{11/2}$ level is thermally populated from the ${}^4S_{3/2}$ level, but as the temperature decreases to 77 K, the energy of thermal quanta and consequently the probability that the ${}^2H_{11/2}$ level is populated decrease as well. This can explain the significant decrease in the relative intensity of the luminescence band around 522 nm at $T = 77$ K.

Going back to the luminescence spectra at 300 K (see Fig. 3, *a*), we can see that the spectrum of the 1.0 % ErF_3 sample has the lowest value of the relative intensity of the luminescence peak caused by the ${}^2H_{11/2} \rightarrow {}^4I_{15/2}$ transition (522 nm) and the highest value for the ${}^4F_{9/2} \rightarrow {}^4I_{15/2}$ transition (660 nm). Notice that the maximum relative intensity of the 660-nm

band was observed in the spectrum of this sample both at room temperature and at 77 K.

A consistent explanation for these facts is as follows. An increase in the dopant concentration leads to a decrease in the average distance between optically active ions and an increased probability of their exchange interaction, which affects the increase in the population of the ${}^4F_{9/2}$ level and a decrease in the relative population of the ${}^2H_{11/2}$ level. The invariable relative intensity of the ${}^4S_{3/2} \rightarrow {}^4I_{13/2}$ transition (850 nm) indicates that the change in the Er^{3+} ion concentration does not lead to a change in the ${}^4S_{3/2}$ level population mechanism.

Let us consider the characteristics of the energy levels ${}^2H_{11/2}$ and ${}^4S_{3/2}$ in more detail. According to the data obtained from the optical absorption spectra, the energy gap ΔE between these levels is about 770 cm^{-1} . Due to such a low value (much less than 2000 cm^{-1}) for glasses doped with Er^{3+} ions, the relative population of the ${}^4H_{11/2}$ and ${}^4S_{3/2}$ levels depends on temperature [19]. Besides, since ΔE exceeds the energy of thermal quanta (about 210 cm^{-1}) at room temperature, the luminescence bands from two energy levels do not overlap. As a result, the upper ${}^2H_{11/2}$ level has a smaller population of optically active ions than the ${}^4S_{3/2}$ level; thus, the ${}^2H_{11/2}$ and ${}^4S_{3/2}$ levels turn out to be thermally coupled, and their relative populations obey the Boltzmann distribution [19].

This phenomenon is used to develop optical temperature sensors based on the FIR (Fluorescence Intensity Ratio) technique [20] requiring for the temperature dependence of the intensity ratio of the thermally coupled levels to be proportional to the relative population of the ${}^2H_{11/2}$ and ${}^4S_{3/2}$ levels [21]:

$$\text{FIR} = \frac{I_H}{I_S} = \frac{g_H \sigma_H \omega_H}{g_S \sigma_S \omega_S} \exp\left(-\frac{\Delta E}{k_B T}\right) = C \exp\left(-\frac{\Delta E}{k_B T}\right), \quad (1)$$

where I_H, I_S are the intensities of the luminescence peaks associated with the ${}^2H_{11/2} \rightarrow {}^4I_{15/2}$ and ${}^4S_{3/2} \rightarrow {}^4I_{15/2}$ transitions, respectively; the parameters $\sigma_H, \sigma_S, \omega_H, \omega_S$ are the emission cross-sections and frequencies of the luminescent transitions ${}^2H_{11/2} \rightarrow {}^4I_{15/2}$ and ${}^4S_{3/2} \rightarrow {}^4I_{15/2}$; g_H, g_S are the degeneracy factors of the ${}^2H_{11/2}$ and ${}^4S_{3/2}$

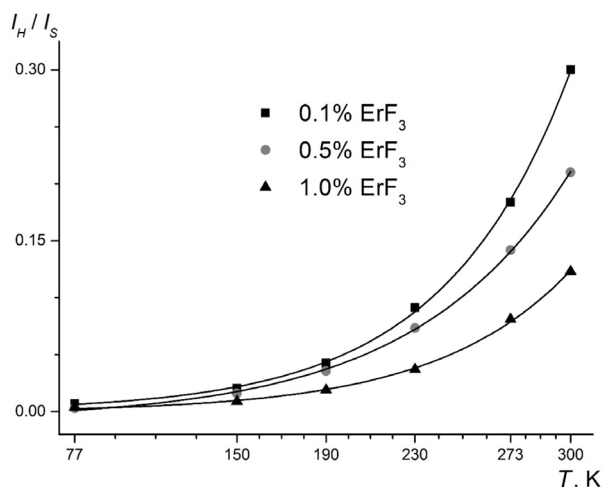


Fig. 4. Experimental FIR (I_H / I_S) results (symbols) for fluoroaluminate glass samples with different concentrations of the dopant Er^{3+} . The solid lines correspond to the exponential approximation by formula (1)

levels; k_B is the Boltzmann constant, and T is the temperature.

To obtain the temperature dependences for FIR of the samples under consideration, we have measured the upconversion luminescence in the temperature range of $77 - 300 \text{ K}$. The experimental data obtained are shown in Fig. 4. We should note that the temperature dependence of the ratio of fluorescence peaks (FIR) is in agreement with the theoretical one and has an exponential character. It can be also seen that FIR increases with increasing temperature for all the samples, indicating an increase in sensitivity. The sample with the lowest Er^{3+} content, 0.1% ErF_3 , has exhibited the highest FIR values in the investigated temperature range, possibly due to a lower probability of exchange interactions of optically active ions and radiation reabsorption, which modify the mechanism of population of the ${}^2H_{11/2}$ and ${}^4S_{3/2}$ levels [11].

The obtained results indicate that the sample with the lowest content of Er^{3+} ions was the most sensitive to temperature changes of all samples with the concentrations of the ErF_3 dopant ranging from 0.1 to $1.0 \text{ mol}\%$.

Conclusion

We have studied the spectral and lumines-



cent properties of fluoroaluminate glasses of the composition $98\text{MgCaSrBaYAl}_2\text{F}_{14}-2\text{Ba}(\text{PO}_3)_2$, doped with the Er^{3+} ions with variable dopant content. Analysis of the optical absorption spectra of the glasses revealed no effects of dopant segregation and no inhomogeneous broadening of the spectral bands in the samples under consideration. The Beer–Lambert–Bouguer law was found to be fulfilled for the most intense absorption bands.

We have obtained the upconversion luminescence spectra at temperatures of 77 and 300 K, and proposed a mechanism for the transfer of excitation energy, explaining the nature of the observed luminescence bands in the visible and near-infrared regions of the spectrum, based on analysis of the energy level diagram of the Er^{3+} ion. The key factor governing the emergence of these bands is the population of the ${}^4F_{7/2}$ energy level, which may occur in two ways: through exchange interaction and through absorption of electromagnetic radiation energy from the excited state.

We have established the influence of the concentration of dopant ions on the relative intensity of the band with a maximum of about 660 nm corresponding to the ${}^4F_{9/2} \rightarrow {}^4I_{15/2}$ electronic transition. The relative intensity growth in this band with an increase in the dopant concentration can be attributed to increasing probability of exchange interaction between optically active ions due to a decrease in the average distance between Er^{3+} ions.

The intensity ratio of the upconversion luminescence bands with maxima around 522 nm and 550 nm in the temperature range of 77–300 K were analyzed using the FIR technique. These bands correspond to transitions from the thermally coupled energy levels ${}^2H_{11/2}$ and ${}^4S_{3/2}$ to the ground state ${}^4I_{15/2}$. The obtained

temperature dependences of the ratio of the fluorescence intensity peaks indicate the exponential character of the relative population of the ${}^2H_{11/2}$ and ${}^4S_{3/2}$ levels. We have additionally found that the FIR value increased and reached its maximum value at 300 K with increasing temperature for all the samples examined. We have also established that the FIR response decreases with an increase in the Er^{3+} ion concentration at the same temperature, which may be associated with an increasing probability of exchange interactions between optically active ions and with radiation reabsorption; these factors lead to a modification of the process of population of the ${}^2H_{11/2}$ and ${}^4S_{3/2}$ levels.

The results of this study indicate that it is possible to use activated fluoroaluminate glasses of the composition we have investigated as a material for creating a sensitive element in optical temperature sensors based on the FIR technique.

Of all the samples examined, the one with the minimal Er^{3+} ion content (0.1%) was the most sensitive to temperature changes in the temperature range of 77–300 K.

Potential use of fluoroaluminate glasses of the investigated composition in the region of high temperatures (up to 600 K) and the reaction of the samples to such temperature changes require further study.

Acknowledgment

The author expresses his most sincere gratitude to V.A. Assev, associate professor of the ITMO University, for assistance in conducting luminescence measurements, and to A.V. Semench, associate professor of the Polytechnic University for fruitful discussion of the results.

REFERENCES

- [1] M.J. Thorpe, K.D. Moll, R.J. Jones, et al., Broadband cavity ringdown spectroscopy for sensitive and rapid molecular detection, *Science*. 311 (5767) (2006) 1595–1599.
- [2] G.F. West, W. Höfle, Spectral attenuation of fluoride glass fibers, *J. Non-Cryst. Solids*. 213–214 (1997) 189–192.
- [3] M.A. Khamis, K. Ennser, Design of highly efficient Pr^{3+} -doped chalcogenide fiber laser, *IEEE Photonics Technology Letters*. 29 (18) (2017) 1580–1583.
- [4] H. Chen, F. Chen, T. Wei, et al., Ho^{3+} -doped fluorophosphate glasses sensitized by Yb^{3+} for efficient 2 μm laser applications, *Opt. Commun*. 321 (2014) 183–188.
- [5] M.C. Paul, S. Bysakh, Sh. Das, et al., Recent developments in rare-earths doped nano-engineered glass based optical fibers for high power fiber lasers, *Trans. Ind. Ceram. Soc.* 75 (4) (2016) 195–208.
- [6] G. Tang, Z. Yang, L. Luo, W. Chen, Dy^{3+} -

doped chalcogenide glass for 1.3- μm optical fiber amplifiers, *J. Mater. Res.* 23 (4) (2008) 954–961.

[7] **J. Fu, M. Kobayashi, S. Sugimoto, J.M. Parker**, Eu^{3+} -activated heavy scintillating glasses, *Mater. Res. Bull.* 43 (6) (2008) 1502–1508.

[8] **M. Haouari, A. Maaoui, N. Saad, A. Bulou**, Optical temperature sensing using green emissions of Er^{3+} doped fluoro-tellurite glass, *Sensors and Actuators, A: Physical*. 261 (2017) 235–242.

[9] **Z.P. Cai, Hue-Yin Xu, S.L. Yang, et al.**, Micrometer-sized point temperature sensor in Er : ZBLALiP, *Proc. SPIE*. 4919 (20 Sept.) (2002) 501–507.

[10] **C.D.S. Brites, P.P. Lima, N.J.O. Silva, et al.**, Thermometry at the nanoscale, *Nanoscale*. 4 (2014) 4799–4829.

[11] **S.F. León-Luis, U.R. Rodríguez-Mendoza, P. Haro-González, et al.**, Role of the host matrix on the thermal sensitivity of the Er^{3+} luminescence in optical temperature sensors, *Sensors and Actuators. B: Chemical*. 174 (2012) 176–186.

[12] **S.A. Sirotkin, D.S. Sysoev, T.V. Bocharova, et al.**, Spectroscopic properties of the glass of fluoroaluminate systems with small additives of barium metaphosphate activated with the ions of rare-earth elements, *Glass Phys. Chem.* 41 (3) (2015) 265–271.

[13] **V.A. Klinkov, A.V. Semencha, E.A. Tsimerman**, Advanced materials for fiber communication systems, Internet of Things, Smart Spaces, and Next Generation Networks and Systems, 17th Intern. Conf., Russia, St. Petersburg,

Aug. 28 –30, 2017. *Proc.*, Springer, Pp. 184–195.

[14] **G.H. Dieke, R.A. Satten**, Spectra and energy levels of rare earth ions in crystals, *Am. J. Phys.* 38 (3) (1970) 399–400.

[15] **A.V. Dmitryuk, G.O. Karapetyan, L.V. Maksimov**, Phenomenon of activator segregation and its spectroscopic consequences, *J. Appl. Spectroscopy*. 22 (1) (1975) 119–141.

[16] **G.S. Landsberg**, *Optika [Optics]*, Moscow, Nauka, 1976.

[17] **A.V. Malov, M.O. Marychev, P.A. Ryabochkina, et al.**, Spektroskopicheskiye i strukturnyye svoystva kristallov kaltsiy-niobiy-galliyevogo granata, aktivirovannykh ionami Er^{3+} [Spectroscopic and structural properties of Er^{3+} -doped calcium-niobium-gallium garnet crystals], *Vestnik Nizhegorodskogo universiteta im. N.I. Lobachevskogo*. (6) (2008) 46–52.

[18] **T. Catunda, L.A.O. Nunes, A. Florez, et al.**, Spectroscopic properties and upconversion mechanisms in Er^{3+} -doped fluorindate glasses, *Phys. Rev. B*. 53 (10) (1996) 6065–6070.

[19] **E. Maurice, G. Baxter, G. Monnom, et al.**, Thermalization effects between upper levels of green fluorescence in Er -doped silica fibers, *Opt. Lett.* 19 (13) (1994) 990–992.

[20] **V.K. Rai**, Temperature sensors and optical sensors, *Appl. Phys. B*. 88 (2) (2007) 297–303.

[21] **V.K. Rai, S.B. Rai**, A comparative study of FIR and FL based temperature sensing schemes: an example of Pr^{3+} , *Appl. Phys. B*. 87 (2) (2007) 323–325.

Received 19.01.2018, accepted 24.01.2018.

THE AUTHOR

KLINKOV Victor A.

Peter the Great St. Petersburg Polytechnic University

29 Politechnicheskaya St., St. Petersburg, 195251, Russian Federation

klinkovvictor@yandex.ru